Excited-state absorption by Eu^{2+} in KBr, KCl, and NaCl

Larry D. Merkle
Physics Department, University of Arkansas, Fayetteville, Arkansas 72701

Pradip K. Bandyopadhyay
Physics Department, Hendrix College, Conway, Arkansas 72032
(Received 30 August 1988)

Excited-state-absorption (ESA) measurement have been made on alkali halide crystals doped with Eu^{2+}, including both as-received and thermally quenched samples. No ESA has been detected in the visible spectral region, but strong excited-state absorption occurs in the near ultraviolet. This is in qualitative agreement with the published excited-state ionization model of ESA in CaF_2:Eu^{2+}. However, the observed ESA onset energies in alkali halides are significantly lower than predicted by that model, and are more nearly consistent with a charge-transfer transition. The ESA spectra show little evidence of ground-state depletion, and together with data on the fluence dependence of fluorescence and laser transmission, this suggests that the quantum efficiency of Eu^{2+} in these hosts is rather low.

I. INTRODUCTION

Although the bulk of research and development work on tunable solid-state-laser materials has centered on systems emitting in the infrared and red spectral regions, it is also of interest to search for materials emitting at shorter wavelengths.[1] The strong, broad pump bands and allowed, vibronically coupled band emission of the divalent europium ion in a sufficiently strong crystalline field make this ion interesting for laser operation in the violet and blue spectral regions.[2,3] However, in CaF_2:Eu^{2+} it was found that strong excited-state absorption throughout the visible region prevented laser action.[4] This absorption was attributed to ionization of Eu^{2+} to Eu^{3+}, an assignment supported by an electrostatic model for photoionization.[5] This raises the possibilty that in appropriately chosen hosts the excited-state-ionization transition may be displaced well into the ultraviolet where it would not affect laser action. According to the electrostatic model, the primary host property needed to achieve this is a small Madelung energy at the europium site.

Alkali halide crystals, in which europium impurities substitute for alkali ions, have appropriately small alkali ion site Madelung energies. The resulting unfavorability of removal of an electron from Eu^{2+} in these hosts may be understood heuristically as due to the large charge mismatch which would result at the normally monovalent alkali ion site. The excited-state-ionization transition in these hosts should lie at energies well above the visible range, permitting a search for intraionic excited-state transitions in the visible and near ultraviolet and evaluation of the potential of divalent europium ions for laser action in appropriate hosts.

In view of this, room-temperature excited-state-absorption (ESA) measurements have been carried out on KCl:Eu, KBr:Eu, and NaCl:Eu crystals. After a description of the experimental details we report the results of these measurements and data on the irradiance dependence of the europium fluorescence and of the transmission of the pump laser. It is found that the degree of excitation and ground-state depletion is smaller at a given irradiance than predicted by a simple saturable absorption model, leading to development of a more complex model of the excitation process. This permits a rough estimate of the cross section of the observed ESA transition to be made, which is followed by consideration of the possible identity of the transition.

II. EXPERIMENTS

The apparatus for the excited-state absorption measurements is outlined in Fig. 1. The sample was pumped by an excimer laser operating on XeF, and hence at 350-nm wavelength. The laser is a Lumonics EX-510 with a pulse duration of about 10 ns and with pulse repetition frequency chosen as 20 Hz for most experiments. The pulse energy was monitored by a Scientech 364 power meter. Spherical and cylindrical lenses were employed to adjust the size and shape of the beam at the sample. As

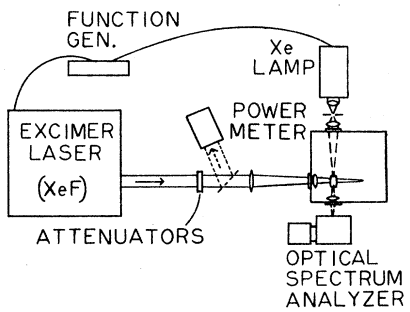

FIG. 1. Apparatus for excited-state absorption.

determined using knife-edge scans, the horizontal beam profile had a typical full width at half maximum of 4 mm and a central region about 2 mm wide of constant fluence, and the vertical profile had a full width at half maximum of 2 mm and a central constant region of about 0.5 mm.

The sample transmission was probed by a beam from a Photochemical Research Associates 6100E pulsed Xe lamp, providing pulses of about 700-ns duration (full width at half maximum). The output beam was passed through a pinhole and then focused into the sample on a path orthogonal to the laser pump beam with a diameter of about 0.5 mm. ESA data were taken with the sample masked to pass only the central 3 mm of the pump beam width, so that the average pump fluence in the probed region was greater than 90% of the on-axis fluence. The probe-beam axis passed through the sample about 0.8 to 1.0 mm behind its front face, so that the pump fluence must be corrected for attenuation through this depth as well as for reflection at the front surface.

The triggering circuit for the pump laser and probe lamp permitted adjustment of the timing, with the peak of the lamp pulse coming as much as 7.5 μs before the laser pulse or as much as 1.1 μs after it. Due to the duration of the probe pulse, the shortest delay time used for ESA measurements was 0.5 μs, for which about 95% of the probe pulse arrives after the pump.

The probe beam was detected and analyzed using a Tracor Northern 6500 optical spectrum analyzer with a nongatable intensified photodioide array. A low-dispersion monochromator was used such that a spectral region about 270 nm wide could be measured simultaneously, and spectra were typically averaged over 500 laser pulses. The collecting lens for the transmitted probe beam was masked to minimize collection of sample fluorescence.

ESA spectra were, however, contaminated by fluorescence and scattered laser light. The spectral region masked by this problem was minimized by subtraction of a "laser-only" spectrum from the spectrum of the probe lamp beam which passed through the laser-pumped sample. The absorbance was calculated using this difference spectrum as the "transmitted" signal.

Normally the effect of excited-state absorption and ground-state depletion would be contained in the difference between the absorbance spectrum for the pumped sample and that for the unpumped sample. However, in our experiments the absorbance spectra contained long-lived (minutes or longer) features indicative of radiation damage. To eliminate contamination of the ESA spectra by this effect, the change in absorbance due to excitation of the europium was found by calculating

$$\Delta A(\mathrm{ESA}, t_d) = A(\mathrm{pumped}, t_d) - A(\mathrm{pumped}, -7.5) \quad (1)$$

which compares the absorbance probed at time t_d after pumping with that 7.5 μs before pumping. Since only the probe timing differs, this subtraction contains the difference between excited and unexcited Eu^{2+} ions, but cancels the effect of the radiation damage absorption. Ground-state-absorption spectra were measured using a Cary 14 spectrophotometer.

The time dependence of fluorescence following excitation by the laser pulse has been monitored using a silicon *p-i-n* photodioide, filters to block the laser wavelength, and a Tektronix 7904 oscilloscope or a boxcar averager. The response time of the system was about 20 ns.

The samples used in this study were cleaved from single crystals of KCl:Eu, KBr:Eu, and NaCl:Eu obtained from the crystal-growth facility at Oklahoma State University. All samples were over one year old, so that the europium ions and their charge compensating vacancies were thoroughly aggregated.[6,7] Some samples were studied in this aggregated state, others were annealed for about 16 h at 600–650 °C and quenched to room temperature on a brass block to break up the aggregates. The ground-state absorption spectra of quenched samples were used to estimate the Eu^{2+} concentrations using published calibration data.[8] These concentrations range from about 10^{18} to 10^{19} cm^{-3}. Neither absorption nor fluorescence spectra show any evidence of Eu^{3+}.

III. DATA

Ground-state-absorption spectra of typical quenched and unquenched samples of KCl:Eu, KBr:Eu, and NaCl:Eu are displayed in Fig. 2. The two strong absorption bands are the

$$4f^7(^8S) - 4f^6 5d\,(t_{2g} \text{ and } e_g)$$

transitions familiar in Eu^{2+}, with t_{2g} being the lower energy of the 5*d* states in an octahedral environment.[9] (A charge compensating vacancy, and other nearby Eu-vacancy pairs in the aggregated samples, destroy this

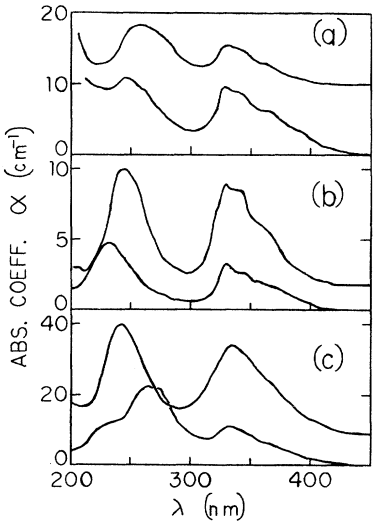

FIG. 2. Ground-state absorption of alkali halides doped with Eu^{2+}, (a): KBr:Eu, (b): KCl:Eu, (c): NaCl:Eu. In each case the lower trace is the absorption of a sample stored at room temperature for over a year and the upper trace is that of a sample annealed overnight at about 650 °C and quenched to room temperature within several hours of measurement. (The baselines are offset for clarity.)

symmetry but the same labels are kept for simplicity.) There is considerable variation in absorption strength from sample to sample, indicating that the Eu^{2+} concentration is not uniform. The spectra for the two chlorides are similar to those reported by those who have studied Eu^{2+} aggregation effects.[6,7] The spectrum of recently quenched KCl:Eu agrees quite closely with Refs. 7 and 8, indicating that the thermal breakup of aggregates was successful and that Eu concentrations inferred from spectra on such samples should be reliable. The relative heights of the two absorption bands in quenched NaCl:Eu are sufficiently similar to those of Refs. 6 and 8 to suggest that concentration estimates are accurate within about 20%. However, the quenched KBr:Eu samples show spectra quite different from Ref. 8, a condition which remains true when the annealing temperature is increased to 675 °C. Thus, the breakup of aggregates appears to have been less successful in this host and Eu concentration estimates from spectra are necessarily crude. The absorption coefficient of the shorter wavelength peak will be used to estimate concentrations in this material, as that peak appears less sensitive to aggregation.[6,7] In KCl:Eu and NaCl:Eu the effect of aggregation on the fluorescence spectra have also been reported.[6,7] Comparison with the fluorescence spectra of samples in the present studies confirm the absorption data, in that quenching appears to have broken up aggregates almost completely in KCl:Eu, somewhat less completely in NaCl:Eu.

No excited-state absorption was detectable in the visible spectral region in these materials, in contrast to the behavior of CaF_2:Eu.[4] Detection limits of the measurements may be estimated as follows. In KCl:Eu the change in absorption coefficient averaged over the region 470–740 nm upon pumping with a fluence of 0.30 J/cm^2 was significantly less than 0.08 cm^{-1}, the limit being imposed by noise in the spectra. The total europium concentration in the sample was about 1.3×10^{18} cm^{-3}. As will become evident herein, the fraction of the ions excited is uncertain, limiting the ability to make an accurate estimate of the limit on the ESA cross section. In a NaCl:Eu sample with a very approximate europium concentration of 5×10^{18} cm^{-3} the detection limit is about 0.23 cm^{-1} for a pumping fluence of 0.16 J/cm^2. (In both cases the fluences quoted are the average fluences at the axis of the probe lamp beam.) In KBr:Eu it has been observed that laser irradiation results in *F*-center formation, which interferes with detection of ESA in the visible region. As a result the detection limit for this material is difficult to determine, but is significantly less stringent than in the other samples.

Excited-state absorption was observed in the ultraviolet. Figure 3, curve *A*, shows the observed change in absorption coefficient due to pumping an unannealed sample of KCl:Eu with a europium concentration of about 1.3×10^{18} cm^{-3}, with the probe pulse peaking 0.5 μs after the pump laser pulse. The absorption coefficient data were obtained from the raw data using Eq. (1) and the 3-mm probe path length through the pumped region of the sample. The spectral region in which data can be extracted is limited by the weakness of the probe lamp and

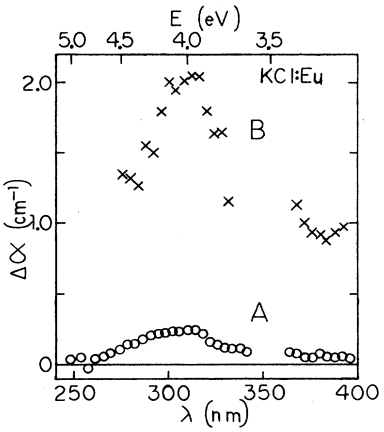

FIG. 3. Change in uv absorption coefficient of KCl:Eu due to pumping. *A*: A never-annealed sample with pumping fluence 0.12 J/cm^2 and total Eu^{2+} concentration 1.3×10^{18} cm^{-3}. *B*: An annealed and quenched sample with pumping fluence 0.18 J/cm^2 and total Eu^{2+} concentration 1.8×10^{18} cm^{-3}. The probe-lamp peak occurred 0.5 μs after the laser pulse.

strong Eu^{2+} absorption at short wavelengths, scattered laser light near 350 nm, and fluorescence for wavelengths longer than about 390 nm. The spectrum observed for a pump delay time of 1.1 μs is similar, with an average magnitude about half that for a 0.5 μs delay, consistent with the observed 1.05 μs fluorescence lifetime of KCl:Eu. This strongly supports the interpretation of the data as due to excited-state absorption.

Similar data are presented in Fig. 3, curve *B*, and in Figs. 4 and 5 for quenched KCl:Eu, unquenched KBr:Eu, quenched KBr:Eu, and quenched NaCl:Eu. The strong ground-state absorption in NaCl:Eu decreased the transmitted probe signal severely, limiting the usable

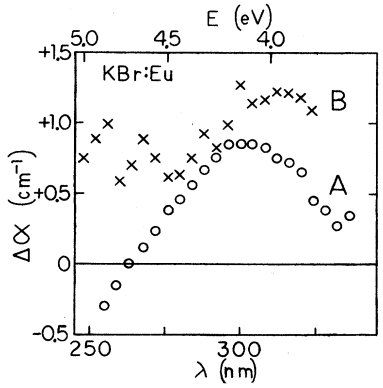

FIG. 4. Change in uv absorption coefficient of KBr:Eu due to pumping. *A*: A never-annealed sample with pumping fluence 0.11 J/cm^2 and total Eu^{2+} concentration an estimated 1.8×10^{18} cm^{-3}. *B*: An annealed and quenched sample with pumping fluence 0.23 J/cm^2 and total Eu^{2+} concentration an estimated 1.1×10^{18} cm^{-3}. The probe-lamp peak occured 0.5 μs after the laser pulse.

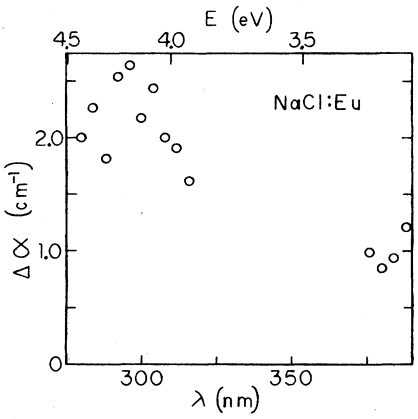

FIG. 5. Change in uv absorption coefficient of an annealed and quenched sample of NaCl:Eu due to pumping. The pumping fluence was 0.065 J/cm^2 and the total Eu^{2+} concentration 9.5×10^{18} cm^{-3}. The probe-lamp peak occured 0.5 μs after the laser pulse.

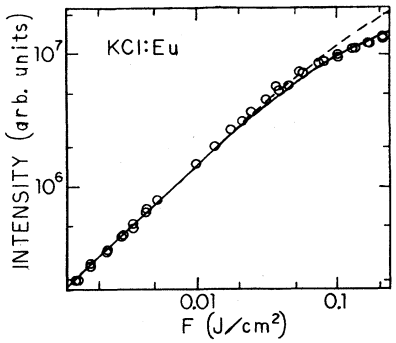

FIG. 6. Log-log plot of integrated fluorescence signal vs fluence for an annealed and quenched sample of KCl:Eu. The dashed curve is Eq. (2) fit to the low-fluence data. The solid curve is Eq. (5), from the model of Fig. 7, with $\sigma_e=2.3\times10^{-18}$ cm^2.

wavelength range in Fig. 5 and preventing the acquisition of any meaningful uv data on unquenched NaCl:Eu. The ratio of signals between a 1.1 μs delay and a 0.5 μs delay between probe and pump pulse peaks is consistent with the fluorescence decay time in each case. Comparison of the quenched and unquenched KCl:Eu samples suggests that the ESA may vary with state of aggregation. However, the sensitivity of the data to noise prevents detailed comparison.

It is notable that these absorption coefficient change data are only very rarely negative. This may indicate that ground-state depletion due to excitation is weak, that is, that the fraction of ions excited is small. To study the dependence of the excited-state population on fluence, the fluorescence has been monitored from the same region of the material interrogated by the probe beam. The region monitored was defined by a mask with 0.6-mm square aperture centered on the probe-beam path. The optical spectrum analyzer scan time, 5 ms, assures that the fluorescence signal is integrated over time, and its software was used to integrate spectrally as well. The resulting total fluorescence signal as a function of the fluence at the probe plane is shown for a quenched KCl:Eu sample in Fig. 6. As a first attempt to fit the data a two-level system is assumed, with stimulated emission from the excited state neglected due to the relaxation which can be expected within the $4f^6 5d$ excited state in a solid. Spontaneous emission is also neglected, due to the brevity of the laser pulse. A rate-equation approach to such a model, assuming a square pump pulse for simplicity, yields the following ratio of excited-state population, n_1, to total Eu^{2+} population, n_t:

$$n_1/n_t=1-e^{-\sigma F/E}. \tag{2}$$

Here σ is the ground-state absorption cross section at 350 nm, which may be extracted from the absorption spectra once the Eu concentration has been estimated using Ref. 8, F is the fluence, and E is the energy of a 350-nm photon. The ratio of fluorescence signal to n_1 is determined by fitting the low-intensity region, resulting in the dashed curve in Fig. 6. It is evident that the fluorescence signal falls below this curve at high fluences, a feature observed for all hosts. Correcting for this shortfall, the fraction of ions predicted to be in the excited state at the end of a pump pulse with the fluence employed in the ESA data of Fig. 3(b) is about 0.5. About 60% of these remain in that state after one-half microsecond, the probe peak arrival time in Fig. 3(b). The resultant bleaching of the ground-state absorption, which may be estimated by referral to Fig. 2, is not evident in the ESA data. Indeed, if such bleaching does occur, the ESA cross section would have to have a wavelength dependence remarkably similar to the ground-state absorption to yield the observed ESA spectrum. As has been noted by Fairbank *et al.*, this gives reason to suspect that the fraction of ions excited is smaller than the predicted 0.3.[10] Similar conclusions may be drawn for quenched KCl:Eu and for KBr:Eu, quenched and unquenched.

As a further check on the degree of excitation, transmission of the pump laser was measured as a function of incident fluence in one unquenched KCl:Eu and several unquenched KBr:Eu samples. In some of these experiments the entire beam was passed through the sample focused to a smaller size than usual and with no mask. For maximum pulse energy in these experiments the peak (beam center) incident fluence was 0.9 J/cm^2 and the average fluence was 0.4 J/cm^2. In one experiment on KBr:Eu the standard beam size was employed and the sample face was masked with a rectangular aperture 3×1 mm centered on the beam so that the sample was exposed to a more nearly uniform fluence to simplify analysis. At maximum pulse energy in this case the peak fluence was 0.28 J/cm^2 and the average fluence was 0.22 J/cm^2. In all cases the transmittance of the sample was found to be independent of incident fluence to within experimental error. Corrected for surface reflection, the transmittance of a 0.7 mm thick KCl:Eu sample was found to be 0.75 ± 0.05 and for a typical 1.0 mm thick KBr:Eu sample it was 0.45 ± 0.05.

DeShazer *et al.*, have recently published a study of saturated absorption in Al_2O_3:Ti, applying the same model

as above to analyze their results.[11] To apply their equation for the fluence dependence of transmission to the preceding results on KBr:Eu, the Eu^{2+} concentration may be estimated from the absorption data and the published calibration[8] to be roughly 1.75×10^{18} cm^{-3} and the 350-nm absorption cross section to be 4.21×10^{-18} cm^2. With a sample thickness of 1.0 mm, Eq. (3) of DeShazer *et al.* predicts a transmittance of 0.48 in the low-fluence limit, but a value of 0.72 for an incident fluence of 0.3 J/cm^2. Strong bleaching of the absorption is also predicted in KCl:Eu and for other reasonable estimates of the concentration in KBr:Eu. The marked disagreement with the observed independence of transmittance on fluence indicates that the europium ions in these hosts are essentially always in a state with strong 350-nm absorption. This is consistent with the lack of bleaching of absorption in the ESA data.

Simple measurements of the fluorescence lifetime of Eu^{2+} in each host have been extracted from oscilloscope traces. The estimated accuracy of these measurements is ±100 ns. The lifetime was found to be about 1.05 μs for both KBr:Eu and KCl:Eu, and 0.75 μs for NaCl:Eu, with no significant difference between quenched and unquenched samples in any host. These values are similar to those published for Eu^{2+} in various hosts, and the weak reported temperature dependences suggest that these lifetimes are close to radiative values.[12,13] The lifetimes were also found to be independent of incident laser fluence, indicating that the sublinear dependence of fluorescence signal on fluence exemplified in Fig. 6 is probably not due to any population dependence of the fluorescence quantum efficiency.

The fluorescence decay measurements yielded one surprising result. The observed rise time of the fluorescence was greater than the 20-ns response time of the detection system, being about 200 ± 50 ns in all cases. Relaxation within the closely spaced states of the $4f^6 5d(t_{2g})$ manifold would normally be expected to be very rapid, and the reason for the observed rise time is unclear.

IV. MODEL FOR DEGREE OF EXCITATION

Before the excited-state absorption spectra can be analyzed further, it is necessary to obtain an estimate of the fraction of ions excited, and the data of the previous section indicate that Eq. (2) is not adequate for this purpose. The fluence dependence of the fluorescence strength indicates weaker than predicted excitation at high fluences, and the ESA data themselves indicate that the fraction excited at a given fluence is probably significantly smaller than the fluorescence data alone suggest. Several possible mechanisms will be considered in order to identify a plausible explanation for these data.

The simplest way to explain the smaller than expected bleaching of the ground-state absorption and the weak fluence dependence of transmittance would be the assumption of a small quantum efficiency for Eu^{2+}. Here this does not refer to a large branching ratio for nonradiative decay by the fluorescent ions, as the time dependence of such decay is reflected in the fluorescence lifetime which is long enough in the present case to permit few decays during the laser pulse. Rather, it envisions the existence of two classes of Eu ions, one class emitting the observed fluorescence upon excitation, the other decaying radiationlessly so rapidly that these ions do not fluoresce and are nearly always in the ground state. There is evidence that a similar situation may exist in other hosts. The quantum efficiency of Eu^{2+} in CaF_2 has been measured to be 0.62, with still lower values in some other hosts, even though the fluorescence lifetimes in these hosts typically are not shorter at room temperature than at low temperature.[13] The existence of a class of ions which do not fluoresce may be due, for example, to the presence of ions in sites with localized vibrational modes which promote strong nonradiative decay or in sites from which efficient energy transfer occurs to rapidly decaying defects. The presence of aggregates of Eu^{2+}-cation vacancy pairs in alkali halides may provide such sites. If a sufficiently small fraction of the ions are in the fluorescent class the ground-state population would remain large enough to explain the very small amount of bleaching observed in the ESA spectra, and the laser transmittance would vary only weakly with fluence. However, this mechanism cannot explain the fluence dependence of the integrated fluorescence signal, as it continues to treat the fluorescent ions just as did the two level model of Sec. III.

The weak growth of the fluorescence at high fluence could be explained, at least qualitatively, by the inclusion of stimulated emission in the model leading to Eq. (2). However, this results in laser transmission growing even more strongly with fluence than in the model of DeShazer *et al.*,[11] clearly at variance with the transmission experiments.

Since excited-state absorption is observed in the ultraviolet a half microsecond after the laser pulse, it is reasonable to attribute the fluence dependence of the integrated fluorescence to the effect of ESA during the laser pulse. It is straightforward to solve a set of rate equations for a three-level model in which ground-state absorption and excited-state absorption occur neglecting stimulated emission and spontaneous decay. The resulting population growth of the first excited state with fluence is indeed weaker than in the two-level model of Sec. III, in qualitative agreement with the data, but the ground-state population is depleted much more strongly than in the earlier model, at variance with the ESA data.

The model may be modified to keep the ground-state population larger by assuming that the final state of the ESA transition undergoes almost instantaneous nonradiative relaxation to the ground state. If excited-state absorption does occur during the laser pulse then the assumption of nonradiative decay of the higher state is reasonable, in that the only fluorescence observed between 220 and 800 nm in these materials is the well-known $4f^6 5d(t_{2g})$-$4f^7$ band. The modified model is sketched in Fig. 7. Level 0 is the ground state with population n_0, level 1 is the $4f^6 5d(t_{2g})$ excited state with population n_1, and level 2 is the terminal state of the excited-state absorption. Since its nonradiative decay to the ground state is presumed to be very rapid, its popula-

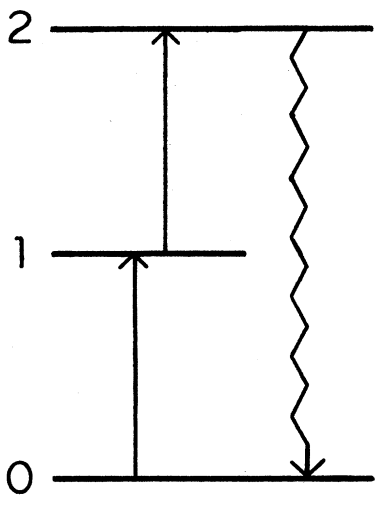

FIG. 7. Model for excited-state absorption and fluence dependence of fluorescence in Eu^{2+}-doped alkali halides.

tion may be taken as zero and the total europium population, n_t, is just n_0+n_1. Therefore if σ_g is the ground-state absorption cross section, σ_e is the excited-state absorption cross section, I is the laser irradiance, and E is the 350-nm photon energy, the rate equations describing the response of this system to laser irradiation are as follows:

$$dn_0/dt = -n_0\sigma_g I/E + n_1\sigma_e I/E \ , \tag{3}$$

$$dn_1/dt = +n_0\sigma_g I/E - n_1\sigma_e I/E \ . \tag{4}$$

If it is assumed for simplicity that the irradiance is constant during the laser pulse and that the pulse fluence is F, then at the end of the laser pulse the fraction of ions in the excited state is

$$n_1/n_t = \frac{\sigma_g}{\sigma_g+\sigma_e}\{1-\exp[-(\sigma_g+\sigma_e)F/E]\} \ . \tag{5}$$

This result may be used to fit the fluence dependence of the integrated fluorescence signal, such as that for quenched KCl:Eu in Fig. 6. Using the low-fluence portion to determine the proportionality of fluorescence to excited fraction and estimating the ground-state-absorption cross section from the published calibration data as usual, the excited-state-absorption cross section may be adjusted to fit the data. The solid curve in Fig. 6 shows that a reasonable fit for this material is obtained with an ESA cross section of 2.3×10^{-18} cm^2. The cross sections obtained from fitting the fluorescence data for all three hosts are given in Table I.

This model may also be checked against the near independence on fluence of laser transmission in KCl:Eu and KBr:Eu. A simple numerical approach was used to calculate the transmission of the laser pulse rather than an analytical solution, as this facilitated modification of the calculation to check various models. The laser pulse was divided into 50 discrete parts such that even for the highest irradiances encountered in the experiments the fluence in each part was small compared to that at which saturation of absorption becomes significant. The sample beam path was divided into 10 slices, each very thin compared to the laser penetration depth in any sample. In this way the transmission of the pulse could be calculated in discrete steps using simplified versions of the rate equations. It was found that for any excited-state-absorption cross section within a factor of 1.5 of the ground-state cross section, the transmittance predicted by the model of Fig. 7 remained within a few percent of its low-fluence value for all experimentally encountered fluences. As Table I shows, for some of the materials studied the ratio of cross sections needed to fit the fluorescence data lies outside this range. Thus, this model alone does not give transmittance predictions consistent with the data in some cases.

It therefore appears necessary to combine the model of Fig. 7 with the assumption of a low quantum efficiency. That is, if a large fraction (typically at least two thirds) of the europium ions are in sites which decay so rapidly as

TABLE I. Comparison of excited-state-absorption cross sections estimated by different means. σ_g is the ground-state cross section at 350 nm inferred from the absorption coefficient and the concentration estimated from the short wavelength absorption peak in quenched samples using the calibration data of Ref. 8. σ_e from fluorescence is the 350-nm excited-state cross section needed in Eq. (5) to fit the fluence dependence of fluorescence. $\langle\sigma_e\rangle$ from ESA is the average excited-state cross section estimated from the ESA data for the stated quantum efficiency (QE).

Sample	σ_g (10^{-18} cm^2)	σ_e from fluorescence (10^{-18} cm^2)	$\langle\sigma_e\rangle$ from ESA with $QE=1$ (10^{-18} cm^2)	QE_{max}	$\langle\sigma_e\rangle$ from ESA with QE_{max} (10^{-18} cm^2)
KCl:Eu (quenched)	2.8	2.3	≈4	0.33	≈10
KCl:Eu (unquenched)	1.8	3.2	≈2	0.33	≈3
KBr:Eu (quenched)	3.3	2.3	≈7	0.25	≈15
KBr:Eu (unquenched)	4.2	9.7	≈5	0.50	≈7
NaCl:Eu (quenched)	2.2	9.8	≈4	0.35	≈9

to virtually always be in the ground state, then the transmittance data become consistent with the cross sections obtained from fluorescence data. Two approaches may be used to estimate the range of quantum efficiencies for which the fluorescence data may be consistent with the excited-state-absorption data. The primary approach is the limitation of the fraction of ions excited to a range in which physically plausible ESA spectra are obtained.[10] An upper limit on the fraction excited is set by the rather implausible similarity of ground- and excited-state spectra predicted for too large values. The ratio of this fraction to that predicted from the integrated fluorescence data then gives an upper limit on the quantum efficiency. In the present case it is difficult to obtain a lower limit on the fraction excited by Fairbank *et al.*'s approach. Figures 8–11 show the ESA cross-section spectra calculated from the data of Figs. 3 and 4 for unit quantum efficiency and for an upper-limit estimate of the quantum efficiency. Figure 12 presents similar spectra for NaCl:Eu, except that here the spectral data are so limited that the preceding criterion is not useful to limit the quantum efficiency, so that the nonunit quantum effiency was simply chosen to be comparable to the other hosts.

A second approach for estimation of the quantum efficiency is comparison of the 350-nm excited-state-absorption cross section predicted by fitting the fluorescence data with the cross section predicted from the ESA data for a given quantum efficiency. This approach is limited, however, by the inability to observe the absorption at 350 nm in the pump-probe measurements and by the fact that ESA during the laser pulse probably originates on a not fully relaxed state, unlike the situation after a delay of 0.5 μs. Even so, this approach may help to place a rough lower limit on the quantum efficiency, since for a very small fraction of ions excited the average ESA cross section in the ultraviolet would become unrealistically large compared to the value which fits the fluorescence data. Table I compares the ESA cross section values from Figs. 8–12, averaged over the detected spectral region, to the values from the fitting of the fluorescence data. For three of the five materials the agreement is reasonable, perhaps as much as can be expected in view of the limitations noted previously.

On the whole it appears that the model proposed here, combining a relatively low quantum efficiency with nonradiative decay of the state reached by excited-state absorption, is reasonable. Each component of the model is plausible, and the overall agreement with experiment is satisfactory.

Now that estimates, albeit crude ones, are available for the quantum efficiency it is possible to estimate detection limits for the ESA measurements in the visible region. For unquenched KCl:Eu the detection limit on the absorption coefficient, 0.08 cm^{-1}, pertains to a fluence of

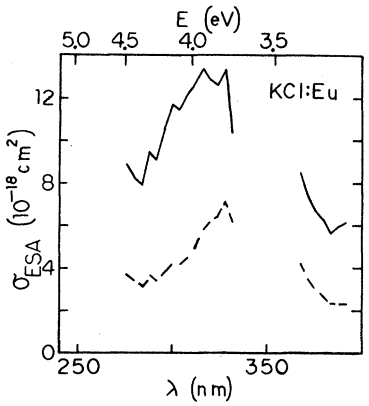

FIG. 9. Excited-state-absorption cross section from the data of Fig. 3 for annealed and quenched KCl:Eu. The dashed curve assumes a quantum efficiency of one, corresponding to a fraction of ions excited of 0.30. The solid curve assumes a quantum efficiency of 0.33.

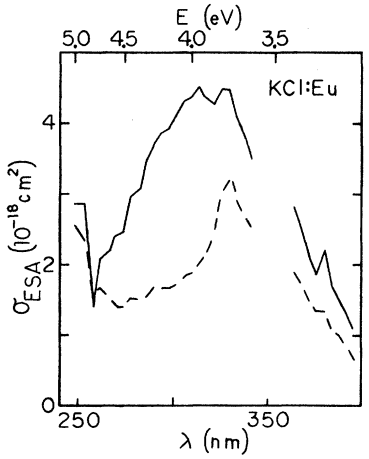

FIG. 8. Excited-state-absorption cross section from the data of Fig. 3 for never-annealed KCl:Eu. The dashed curve assumes a quantum efficiency of one, corresponding to a fraction of ions excited of 0.15. The solid curve assumes a quantum efficiency of 0.33.

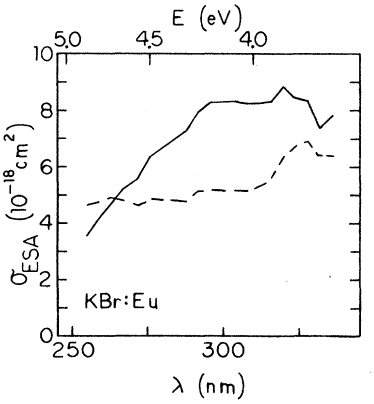

FIG. 10. Excited-state-absorption cross section from the data of Fig. 4 for never-annealed KBr:Eu. The dashed curve assumes a quantum efficiency of one, corresponding to a fraction of ions excited of 0.15. The solid curve assumes a quantum efficiency of 0.50.

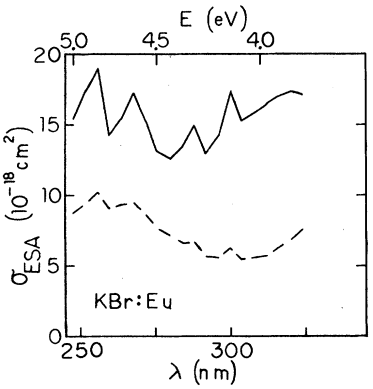

FIG. 11. Excited-state-absorption cross section from the data of Fig. 4 for annealed and quenched KBr:Eu. The dashed curve assumes a quantum efficiency of one, corresponding to a fraction of ions excited of 0.30. The solid curve assumes a quantum efficiency of 0.25.

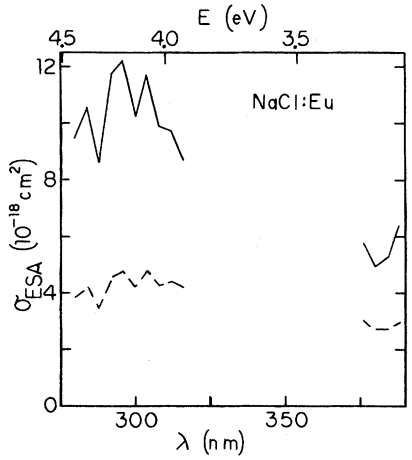

FIG. 12. Excited-state-absorption cross section from the data of Fig. 5 for annealed and quenched NaCl:Eu. The dashed curve assumes a quantum efficiency of one, corresponding to a fraction of ions excited of 0.07. The solid curve assumes a quantum efficiency of 0.35.

0.3 J/cm^2. Combining the fluorescence data with the rough estimate of quantum efficiency, 0.33, from Table I and Fig. 8, the fraction of ions excited 0.5 μs after excitation is estimated to be 0.07. Since the ground-state absorption of this sample after a subsequent thermal anneal and quench yielded a total concentration of about 1.3×10^{18} cm^{-3}, the resulting detection limit on the average ESA cross section in the visible is about 1×10^{-18} cm^2. Similar calculations for NaCl:Eu yield the same approximate detection limit. Although this is not a particularly stringent limit, it is almost a factor of 20 weaker than the visible excited-state absorption reported in CaF_2:Eu^{2+} by Owen, *et al.*[4]

V. INTERPRETATION OF EXCITED-STATE-ABSORPTION SPECTRA

The primary features of the excited-state-absorption spectra in europium-doped alkali halides are a lack of observable absorption in the visible region and rather strong, broad absorption in the near ultraviolet. The ionization model developed by Pedrini *et al.*,[5] and adapted by Owen *et al.*,[4] may be applied to Eu^{2+} in the alkali halides for comparison with the observed spectra. In this model the onset energy for excited-state ionization, E_{ESI}, is given by

$$E_{ESI}=I_3-E_M+E_p-E_{exc}-dE_M(\mathrm{NN})\ . \tag{6}$$

Here, I_3 is the third ionization potential of europium, 24.92 eV (Ref. 14) and E_M is the Madelung energy of an electron at the cation site in which the impurity resides, calculated from data in standard solid state texts and corrected for the charge compensating vacancy on a nearest-neighbor cation site.[15] The resulting E_M values are 11.24 eV in KCl, 12.56 eV in NaCl, and 10.7 eV in KBr. E_p is the host polarization contribution to the energy, which is -1.92 eV for KCl (Ref. 16) -2.5 eV for NaCl,[17] and will be assumed to be about -2 eV for KBr. E_{exc} is the excitation energy of the impurity, estimable from the spectra, and dE_M(NN) is the change in the Madelung energy due to the fact that the neighboring ions around the impurity probably have different equilibrium positions from those around the host cation. No data exist to determine this term directly, so two estimates are presented in Table II. One assumes the neigh-

TABLE II. Onset energies for excited-state absorption by ionization using Eq. (6). E_{ESI} for R_{NN} (host) is the onset energy calculated assuming the neighbors to the Eu^{2+} have the same positions as in the pure host crystal. dE_M(NN) and E_{ESI} for $R_{NN}(EuX_2)$ are the correction to the Madelung energy and the ionization onset energy, respectively, assuming the distance between the Eu^{2+} and the nearest-neighbor halogens is the corresponding average distance in EuX_2, corrected for the coordination number dependence of the cation radius.

Sample	E_{ESI} for R_{NN}(host) (eV)	dE_M(NN) for $R_{NN}(EuX_2)$ (X=halogen) (eV)	E_{ESI} for $R_{NN}(EuX_2)$ (X=halogen) (eV)
KCl:Eu	8.5	+1.8	6.7
KBr:Eu	9.0	+2.0	7.0
NaCl:Eu	6.6	−1.4	8.0

bors retain the same positions as in the pure host crystal, the other uses the nearest-neighbor-anion–europium distance in the stoichiometric europium dihalide, corrected for the dependence of effective cation radius on coordination number.[18,19]

The resulting values for E_{ESI} are given in Table II. Evidently the model would predict the onset of excited state ionization to occur well into the ultraviolet for any reasonable choice of nearest-neighbor-anion position. Indeed, these energies are comparable to the band-gap energies in these three hosts, which may indicate that the model has overestimated the divalent-to-trivalent ionization energy since it places the Eu^{2+} ground state in the host valence band.[20] It is notable, however, that the electrostatic ionization model has generally yielded predictions accurate to within about an eV for a variety of rare-earth impurities in other hosts.[4,21]

It is therefore appropriate to consider intraionic transitions as possible explanations of the excited state absorption. The metastable state of Eu^{2+} in an octahedral site of relatively strong crystal field, which adequately approximates the case for all the hosts in this study, is a $S=\frac{7}{2}$ state of the $4f^6(^7F)5d(t_{2g})$ manifold.[22] The observed ESA peaks at about 320 nm, together with metastable state zero phonon energies of about 24 000 cm^{-1},[12] place the ESA final state about 55 000 cm^{-1} above the ground state. Based on the ground-state-absorption spectra, this is above the energy to be expected for the $S=\frac{7}{2}$ states of the $4f^6(^7F)5d(e_g)$ manifold, such that if the observed transition occurs within the $4f^6 5d$ configuration it must terminate on a state of lower spin.[4] It is unlikely that the large excited-state-absorption cross sections estimated in the previous section would be due to such a transition, since to first approximation it is forbidden by both parity and spin. Transitions to excited $4f^7$ states would be parity allowed, though it is not clear whether any of these states lie at the correct energy since the positions of the states above ^6D_J are not known.[23,24] In any case, such transitions would be spin forbidden to first approximation. It is also possible that $4f^6(^7F)6s$ states may lie in the relevant energy range, though transitions to these states would also be parity forbidden in an octahedral field.[4] Although spin-orbit coupling in such a large ion as europium is significant and the presence of a charge compensating vacancy near the Eu^{2+} breaks the octahedral-site symmetry, the observed ground-state absorption spectra indicate that the spin and parity selection rules are followed fairly well in these materials. Therefore, it appears unlikely that any of these intraionic transitions can explain the observed strong excited-state absorption.

Another possible explanation for the observed ESA is charge transfer. Such transitions often occur in the ultraviolet, and are often quite strong.[25] As a rule one expects the lowest-energy charge transfer transition to move an electron from a neighboring anion to the impurity cation. A rough estimate of the transition energy may be made by an approach similar to the electrostatic model for ionization, modified by the inclusion of the excitation energy for application to ESA,[5,25]

$$E_{\mathrm{ESCT}}=I_h-I_2+E_M(\mathrm{Eu})+E_M(h)-E_C-E_{\mathrm{exc}}\ . \tag{7}$$

Here E_{ESCT} is the onset energy for excited-state absorption by charge transfer. I_h is the electron affinity of the halogen, 3.61 eV for chlorine and 3.36 eV for bromine.[26] I_2 is the second ionization potential of europium, 11.24 eV (Ref. 14) and E_C is the magnitude of the Coulomb energy due to attraction between the additional negative charge on the europium site and the additional positive charge on the halogen site after transfer. E_{exc} is the excitation energy of the metastable state of Eu^{2+}. The Madelung energies of the europium site, $E_M(\mathrm{Eu})$, and the halogen, $E_M(h)$, both enter as positive quantities since the electron is transferred from a site where negative charge is favored to a site where positive charge is favored. $E_M(\mathrm{Eu})$ is calculated just as in the ionization model, but for $E_M(h)$ it must be noted that various anions adjacent to the impurity lie at different distances from the charge compensating vacancy. Since this calculation is crude in any case, the result is only given for one particularly simple case, that in which the donor anion is one of the two which have the vacancy as well as the impurity as nearest neighbors. In this case the effects of these missing and excess positive charges cancel, so that $E_M(h)$ becomes equal to that for the perfect lattice. (This calculation makes no attempt to correct for the probable displacement of neighbors around the impurity.) As a result, E_{ESCT} is predicted to be 5.8 eV for NaCl:Eu, 4.0 eV for KCl:Eu, and 3.1 eV for KBr:Eu. Considering the simplicity of the approach, the agreement with the observed excited-state absorption is quite reasonable. Charge transfer may therefore be regarded as the most likely explanation of the ESA data.

VI. CONCLUSION

The absence of detectable excited-state absorption in the visible spectral region in europium-doped alkali halides indicates that the absorption reported in CaF_2 was indeed a host-sensitive effect, and that it is premature to rule out Eu^{2+} as a tunable solid-state-laser ion. However, the strong ESA in the same spectral region as the pump bands and the apparently low quantum efficiency of the europium indicate that these hosts are not well suited to Eu^{2+} laser operation.

Investigations of Eu^{2+} in other hosts are being prepared to better characterize the excited-state absorption. This should help to test the proposed charge transfer origin of the ESA transition and to determine whether hosts can be found in which laser action is feasible.

ACKNOWLEDGMENTS

The authors wish to thank Stephen Fenno for his help in taking some of the data. This work was supported by a grant from the Arkansas Science and Technology Authority.

[1]*Tunable Solid-State Lasers II,* edited by A. B. Budgor, L. Esterowitz, and L. G. DeShazer (Springer, Berlin, 1986).
[2]Walter E. Bron and Max Wagner, Phys. Rev. **145**, 689 (1966).
[3]G. Blasse, Phys. Status Solidi B **55**, K131 (1973).
[4]James F. Owen, Paul B. Dorain, and Takao Kobayasi, J. Appl. Phys. **52**, 1216 (1981).
[5]Christian Pedrini, Donald S. McClure, and Charles H. Anderson, J. Chem. Phys. **70**, 4959 (1979).
[6]F. J. Lopez, H. Murrieta S., J. Hernandez A., and J. Rubio O., Phys. Rev. B **22**, 6428 (1980).
[7]J. Rubio O., H. Murrieta S., J. Hernandez A., and F. J. Lopez, Phys. Rev. B **24**, 4847 (1981).
[8]J. Hernandez A., W. K. Cory, and J. Rubio O., J. Chem. Phys. **72**, 198 (1980).
[9]R. Reisfeld and A. Glasner, J. Opt. Soc. Am. **54**, 331 (1964).
[10]W. M. Fairbank, Jr., G. K. Klauminzer, and A. L. Schawlow, Phys. Rev. B **11**, 60 (1975).
[11]L. G. DeShazer, J. M. Eggleston, and K. W. Kangas, Opt. Lett. **13**, 363 (1988).
[12]Larry D. Merkle, Richard C. Powell, and Timothy M. Wilson, J. Phys. C **11**, 3103 (1978).
[13]Takao Kobayasi, Stanley Mroczkowski, James F. Owen, and Lothar H. Brixner, J. Lumin. **21**, 247 (1980).
[14]W. C. Martin, Lucy Hagan, Joseph Reader, and Jack Sugar, J. Phys. Chem. Ref. Data **3**, 771 (1974).
[15]Francis K. Fong, Robert L. Ford, and Richard H. Heist, Phys. Rev. B **2**, 4202 (1970).
[16]E. S. Rittner, R. A. Hutner, and F. K. Dupre, J. Chem. Phys. **17**, 198 (1949).
[17]T. I. Liberberg-Kucher, Zh. Eksp. Teor. Fiz. **30**, 724 (1956) [Sov. Phys.—JETP **3**, 580 (1956)].
[18]Ralph W. G. Wyckoff, *Crystal Structures,* 2nd ed. (Wiley, New York, 1963).
[19]Stanley K. Dickinson, Air Force Cambridge Research Laboratories Physical Sciences Research Paper No. 439 (1970).
[20]*American Institute of Physics Handbook,* edited by Dwight E. Gray (McGraw-Hill, New York, 1972), p. 9-16.
[21]C. Pedrini, F. Rogemond, and D. S. McClure, J. Appl. Phys. **59**, 1196 (1986).
[22]L. L. Chase, Phys. Rev. B **2**, 2308 (1970).
[23]M. C. Downer, C. D. Cordero-Montalvo, and H. Crosswhite, Phys. Rev. B **28**, 4931 (1983).
[24]M. Casalboni, R. Francini, U. M. Grassano, and R. Pizzoferrato, Phys. Rev. B **34**, 2936 (1986).
[25]Donald S. McClure, in *Optical Properties of Ions in Solids,* edited by Baldassare Di Bartolo (Plenum, New York, 1974), p. 401.
[26]*Handbook of Physics and Chemistry,* 65th ed., edited by Robert C. Weast (CRC, Boca Raton, 1984), p. E-62.